Volume 57(5): 437–447, 2009
Journal of Histochemistry & Cytochemistry
http://www.jhc.org

ARTICLE

3D Visualization and Measurement of Capillaries Supplying Metabolically Different Fiber Types in the Rat Extensor Digitorum Longus Muscle During Denervation and Reinnervation

Jiří Janáček, Vita Čebašek, Lucie Kubínová, Samo Ribarič, and Ida Eržen

Department of Biomathematics, Institute of Physiology, Academy of Sciences of the Czech Republic, Prague, Czech Republic (JJ,LK), and Institute of Anatomy (VČ,IE) and Institute of Pathophysiology (SR), Faculty of Medicine, University of Ljubljana, Ljubljana, Slovenia

SUMMARY The aim of this study was to determine whether capillarity in the denervated and reinnervated rat extensor digitorum longus muscle (EDL) is scaled by muscle fiber oxidative potential. We visualized capillaries adjacent to a metabolically defined fiber type and estimated capillarity of fibers with very high oxidative potential (O) vs fibers with very low oxidative potential (G). Capillaries and muscle fiber types were shown by a combined triple immunofluorescent technique and the histochemical method for NADH-tetrazolium reductase. Stacks of images were captured by a confocal microscope. Applying the *Ellipse* program, fibers were outlined, and the diameter, perimeter, cross-sectional area, length, surface area, and volume within the stack were calculated for both fiber types. Using the Tracer plug-in module, capillaries were traced within the three-dimensional (3D) volume, the length of capillaries adjacent to individual muscle fibers was measured, and the capillary length per fiber length (Lcap/Lfib), surface area (Lcap/Sfib), and volume (Lcap/Vfib) were calculated. Furthermore, capillaries and fibers of both types were visualized in 3D. In all experimental groups, O and G fibers significantly differed in girth, Lcap/Sfib, and Lcap/Vfib, but not in Lcap/Lfib. We conclude that capillarity in the EDL is scaled by muscle fiber size and not by muscle fiber oxidative potential. **(J Histochem Cytochem 57:437–447, 2009)**

KEY WORDS
3D visualization
capillaries
denervation
muscle fiber types
reinnervation

CONFLICTING RESULTS about the relation of the density of capillary network and muscle fiber oxidative potential exist in the literature. Early studies supported the idea that muscle fibers with a high oxidative potential are generally associated with a denser capillary network (Romanul 1965; Romanul and Pollock 1969; Brown et al. 1976; Andersen and Henricksson 1977). This would mean that highly oxidative fibers require a higher rate of oxygen delivery than non-oxidative fibers; therefore, they must be better supplied with a capillary network.

Different reports were based on different methods that were applied for the demonstration of capillaries and for their quantitative estimation (Plyley and Groom 1975; Škorjanc et al. 1998; Hepple and Mathieu-Costello 2001; Hepple and Vogel 2004; Degens et al. 2006). Briefly, some staining methods showed fewer capillaries than others. Counting capillary profiles in two dimensions (2D) can be biased compared with the stereological approach (Mathieu et al. 1983; Kubínová et al. 2001) or to the length estimation by tracing capillaries in three dimensions (3D) (this study). Several parameters were used to describe capillary supply in a muscle. Some of them did not directly take into account fiber size, such as capillary-to fiber ratio (C/F), capillary density (CD; number of capillary profiles per μm^2), number of capillary profiles around a fiber (CAF), and length of capillaries per muscle volume (JV), whereas others did, such as number of capillary profiles per fiber in relation to the fiber cross-sectional area (Capo and Sillau 1983; Degens et al. 2006), local capillary to fiber ratio (LCFR) (Degens et al. 1992; Ahmed et al. 1997; Egginton 2002), CFD (capillary – fiber density = LCFR divided by cross-sectional area of that fiber type) (Degens et al. 1992), length of capillaries per fiber surface area (Lcap/Sfib), length of capil-

Correspondence to: Ida Eržen, Institute of Anatomy, Faculty of Medicine, University of Ljubljana, Korytkova 2, SI-1000 Ljubljana, Slovenia. E-mail: ida.erzen@mf.uni-lj.si

Received for publication October 9, 2008; accepted December 19, 2008 [DOI: 10.1369/jhc.2008.953018].

0022-1554/09/$3.30

laries per fiber volume (Lcap/Vfib) (Kubínová et al. 2001), number of capillary profiles per 1000 μm^2 of fiber area (CCA) (Panisello et al. 2008), and others.

The relation between the intensity of the oxidative metabolism and "capillary density" has been addressed in several studies (Gray and Renkin 1978; Maxwell et al. 1980; Škorjanc et al. 1998; Egginton and Hudlicka 2000; Egginton 2002; Hepple and Vogel 2004; Degens et al. 2006), whereby different muscles from different animals were studied under different experimental conditions.

According to the results obtained in rabbit (Gray and Renkin 1978; Ziada et al. 1984) and rat muscles (Large and Tyler 1985), capillary to fiber ratio for fast oxidative and slow oxidative fibers was larger than those for fast glycolytic fibers within the same muscle. Additionally, in muscles made of fast glycolytic fibers, it was reported that capillary growth occurred without an increase in oxidative capacity or capillary growth preceded the increase in oxidative capacity (Cotter et al. 1973; Brown et al. 1976; Škorjanc et al. 1998). Moreover, Sillau (1985) estimated capillary to fiber ratio and mean and maximal diffusion distances in rat soleus and gastrocnemius muscles that underwent experimental hypothyroidism and reported lack of changes in capillarity despite significant changes in oxidative capacity.

Furthermore, an increased density of the capillary network estimated by the number of capillary profiles per square millimeter (C/D) and capillary to fiber ratio (C/F) was shown in experimental conditions where the increased capacity of the muscles to use O_2 was most probably related to an increased O_2 consumption, e.g., exercise (Mai et al. 1970; Brodal et al. 1977; Ingjer 1979; Adolfson et al. 1981), chronic cold exposure (Sillau et al. 1980), or chronic electrical stimulation (Brown et al. 1976).

Capillary density did not always correlate with oxidative capacity or maximal blood flow (Maxwell et al. 1980). Capo and Sillau (1983) reported that, after triiodothyronine administration, capillarity increased in both rat soleus and white area of the medial head of gastrocnemius muscle, whereas the oxidative capacity increased in the soleus only. Increased oxygen consumption does not necessarily provoke changes in the capillary density (Poole et al. 1989), but it could cause an increase in microvessel tortuosity (Charifi et al. 2003).

This all indicates that oxidative capacity is not the only factor that determines capillarity in skeletal muscles. Accumulation of anaerobic waste products may stimulate an increased capillary supply in glycolytic regions of rat skeletal muscles that is not accompanied by changes in oxidative metabolism (Gute et al. 1994; Egginton and Hudlicka 2000; Badr et al. 2003). Already, Plyley and Groom (1975) showed that the mean number of capillary profiles around a fiber was similar for red and white muscles and hypothesized that differences in capillary density are primarily a consequence of fiber size. Sullivan and Pitman (1984) suggested from the area per capillary values that capillaries around glycolytic fibers must supply oxygen and nutrients to a greater volume of a muscle fiber than capillaries serving oxidative fibers. In human muscles, Ahmed et al. (1997) showed a positive correlation between LCFR and fiber area that was independent of fiber type. The slopes for the regression with fiber type (LCFR vs fiber area) were very close, although mean values were scaled with fiber type oxidative capacity, i.e., I > IIA > IIX.

Several factors have been reported to determine capillarity in skeletal muscles. Unfortunately, different experimental models make it difficult to assess the relative contribution of fiber size, muscle activity, and fiber oxidative capacity to muscle fiber capillarity. A single experimental model, where the contribution of all influential factors to capillarity could be evaluated separately under the same conditions, would be useful. Although the rat extensor digitorum longus (EDL) muscle is classified as a fast, anaerobic muscle, it contains oxidative and non-oxidative fibers that differ in their cross-sectional area (Egginton 1990). This variety of fiber types makes EDL a good model for studying changes in muscle fiber capillarity by fiber type and fiber size under experimental conditions such as denervation and reinnervation. Acute denervation and early reinnervation of the rat EDL muscle is accompanied by profound changes in muscle activity, muscle fiber oxidative potential, fiber size, and fiber type composition.

The aim of this study was to determine whether capillarity in the denervated and reinnervated EDL is scaled by muscle fiber oxidative potential. To achieve this goal, we applied new methods that enabled visualization of capillaries in 3D adjacent to histochemically defined muscle fiber types, as well as measurement of changes in the geometrical characteristics of the capillary network supplying oxidative and non-oxidative fibers in rat EDL muscle that underwent acute denervation and early reinnervation.

Materials and Methods

Experimental Design

Fifteen adult Wistar rats (average body weight: 230 ± 20 g) were divided at random into three groups: denervated (D; nerve-cut), reinnervated (R; nerve-crush), and sham-operated (C; control). Surgery was performed under general anesthesia with Rompun (2% solution; Bayer Vital, Leverkusen, Germany) and Ketanest (10 mg/ml; Parke-Davis GmbH, Berlin, Germany). In all three groups, the skin on the rat back was cut over the left hip to expose the sciatic nerve. No further surgical procedures were performed in the controls, and the wounds were closed

with steel clips. In Group D, the left sciatic nerve was cut, whereas in Group R, the nerve was crushed for 1 min with a serrated hemostat (Ribarič et al. 1991). To prevent reinnervation, a 2-cm segment was excised from the distal part of the cut sciatic nerve in Group D. We used the same denervation protocol as published in Ribarič et al. (1991). Reinervation after nerve crush, defined by a percentage of motor endplates with axon terminals present, was complete on day 28 after nerve crush because the number of visualized motor end plates in EDL muscle samples with axon terminals present was already 100% on day 21 after nerve crush denervation (Ribarič et al. 1991). Control and experimental animals were kept isolated in very small cages where their movement was limited to promote wound healing. Five animals in Groups D and C were bled to death under deep ether anesthesia on day 14 after surgery, and five animals from Group R were bled to death under deep ether anesthesia on day 28 after nerve lesion. The complete EDL muscle was excised from left hind limb of animals in all groups and weighed before being frozen in liquid nitrogen. The Veterinary Administration of the Ministry for Agriculture, Forestry and Food, Republic of Slovenia, approved all experimental procedures (Permit 326-07-285/99).

IHC and Histochemistry

Muscle samples were frozen in liquid nitrogen. Whole 180-μm-thick transverse sections of EDL muscle were cut with the Cryo-Star HM 560 (MICROM International GmbH; Walldorf, Germany) from the middle of the muscle belly, fixed in cold 2% paraformaldehyde for 2 hr, and washed in PBS with addition of 0.2% Triton X-100 (PBS-T).

The triple immunofluorescent staining protocol (Čebašek et al. 2004) was used for visualization of capillaries and muscle fibers. All antibodies were diluted in PBS-T with 3% preimmune rat serum. Floating sections were preincubated in goat serum (1:5) for 30 min. First primary mouse anti-rat CD31 antibody (1:3000; BD Biosciences PharMingen, Franklin Lakes, NJ) was applied for 3 days at 4C to label endothelial cells in capillaries. After thorough rinsing in PBS-T, secondary goat anti-mouse antibodies Alexa Fluor 488 (1:350; Molecular Probes Invitrogen, Carlsbad, CA) were applied for 2 hr to visualize capillaries in green. Second primary mouse anti-human laminin antibody (1:1000; CHEMICON Millipore, Billerica, MA) was applied for 3 days at 4C. After the final rinsing in PBS-T, secondary goat anti-mouse antibody Alexa Fluor 546 (1:350; Molecular Probes) was applied for 2 hr to visualize basal laminas in red. After thorough washing in PBS-T, sections were incubated with fluorescein-labeled Griffonia (bandeira) simplicifolia lectin (GSL I; 1:300 for 2 hr at 4C; Vector Laboratories, Burlingame, CA) (Čebašek et al. 2004).

To differentiate fibers according to their prevailing type of metabolism, the already immunofluorescently stained samples were immersed briefly into the medium for the histochemical reaction to NADH-tetrazolium (TR) (Novikoff et al. 1961), an enzyme representing oxidative metabolism of muscle fibers. Fibers were differentiated into fibers with high oxidative activity (O), intermediate activity (OG), and very low activity (G).

Confocal Microscopy

Stacks of images were captured by the two-channel Zeiss LSM 510 confocal microscope (Carl Zeiss; Jena, Germany) using a Zeiss Plan-Neofluar oil immersion ×40 objective (NA: 1.3). Green and red fluorescences were excited with argon (488 nm) and He/Ne (543 nm) lasers. Emission signal was filtered using a narrow band (505–530 nm) and an LP 560-nm filter. To recognize capillaries surrounding oxidative or non-oxidative fibers, respectively, the NADH histochemical reaction was captured simultaneously in the third channel, applying transmission microscopy. Completely registered stacks (225 × 225 × 20 μm) of images 1 μm apart were captured at 512 × 512-pixel resolution.

Image Analysis and 3D Rendering

Images within individual stacks were pre-processed applying stack contrast adjustment, axial contrast, and a 3D Gaussian filter (plug-ins of the *Ellipse* program). Furthermore, the capillaries were traced interactively in 3D using visualization of the confocal image stack in three orthogonal sections (Figures 1A and 1B) so that each capillary segment was represented by a chain of line segments in 3D. The length of the capillaries was calculated by summing up the lengths of corresponding line segments.

Muscle fiber outlines were interactively drawn in the topmost and bottom image of the stack. The outlines were used for calculation of the fiber cross-sectional area, diameter, and perimeter, as well as for assignment of the capillaries to individual fibers (Figure 1C).

The neighborhood of the fiber was represented by triangulated surface spanning contours obtained by dilation of contours of the fiber cross-section in the top and bottom images by 5 μm. The triangulated surface was selected by a dynamic programming algorithm from triangulated surfaces spanning the contours as the surface encompassing maximal volume (Figure 1D). The total length of the capillaries around each individual muscle fiber was calculated by summing up the lengths of the line segments inside the fiber neighborhood.

Capillaries were assigned to a fiber when they were present within the 5-μm neighborhood from the fiber. Several capillaries could be assigned to two or more fibers. We selected only the highly oxidative fibers and

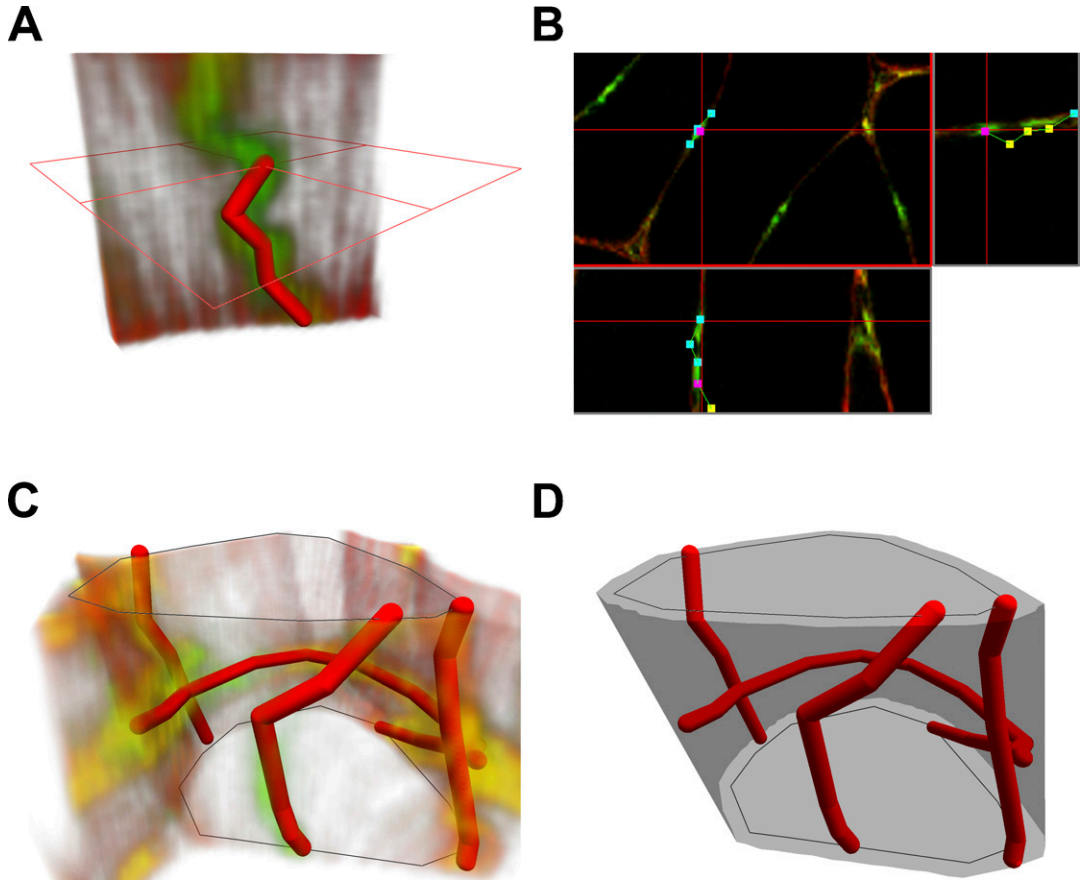

Figure 1 Tracing capillaries, visualization, and measurement of fibers and capillaries from three-dimensional (3D) images acquired by confocal microscopy. (**A**) Capillaries are modeled by linear segments chains. The length of each individual capillary is calculated by summing up the length of linear segments in the chain. (**B**) Tracing the capillary in 3D image volume by Tracer plug-in module: three orthogonal sections through the image stack are shown together with the segments, and a new segment is added by selecting its endpoint using a mouse cursor. (**C**) Muscle fibers are described by contours on the uppermost and lowermost images in the stack. (**D**) A neighborhood of the fiber is constructed as a triangulated surface spanning the dilated contours. The triangulated strip connecting the upper and lower contours encompassing maximal volume is calculated by dynamic programming. Total length of the capillaries adjacent to the fiber is calculated by summing up the lengths of capillaries inside the neighborhood of the fiber.

non-oxidative fibers, respectively, and capillaries within their 5-μm neighborhood.

The geometrical structures modeling the capillaries and fibers were visualized using OpenGL (SGI; Sunnyvale, CA). The capillaries were visualized as chains of cylinders connected by balls, and the fiber surfaces were visualized as triangles. The fibers were assigned a color code according to their type.

Tracing, calculations, and visualizations were done using custom-made modules (Tracer, CapFibers, Contours) of the *Ellipse* program (ViDiTo; Košice, Slovakia).

Statistics

The results were statistically analyzed in SYSTAT (Evanston, IL). Mean values of cross-sectional area, diameter, perimeter, Lcap/Lfib, Lcap/Sfib, and Lcap/Vfib for O and G fibers were calculated within control, denervated, and reinnervated muscles. Differences between O and G fibers within an experimental group were tested by the paired *t*-test.

The relationships between fiber cross-sectional area and Lcap/Vfib, as well as fiber perimeter and Lcap/Sfib, were estimated by regression analysis.

Results

Visualization of capillaries and fiber types in control, denervated, and reinnervated EDL muscle and a 3D rendering of capillaries around fibers with different level of oxidative metabolism are presented in Figure 2.

Highly oxidative fibers (O) were significantly smaller than non-oxidative, presumably glycolytic fibers (G) in control, denervated, and reinnervated EDL muscle in

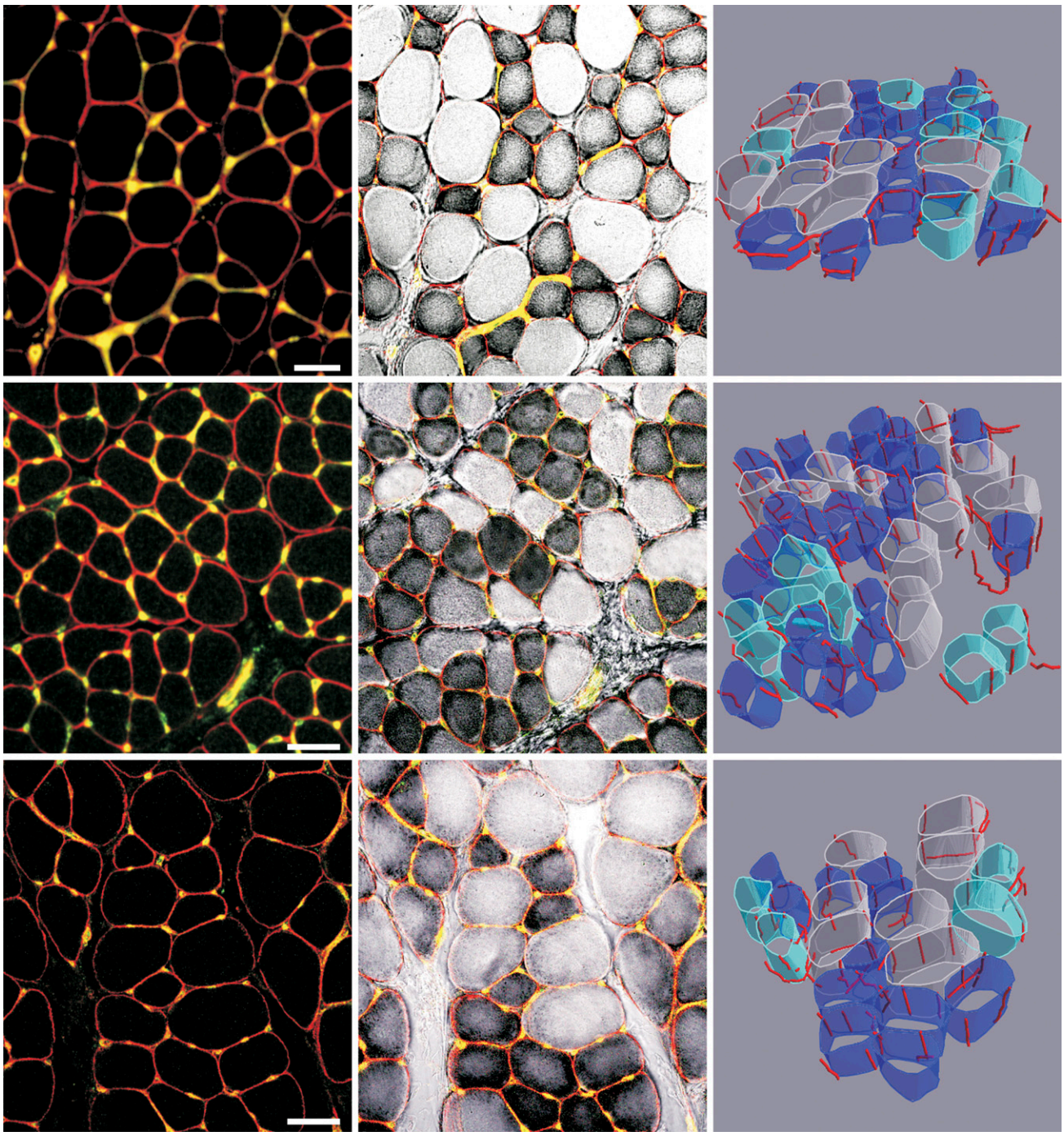

Figure 2 Capillaries and muscle fibers in the rat extensor digitorum longus (EDL) muscle underwent denervation and early reinnervation. Left column: Immunofluorescent demonstration of capillaries and muscle fibers in a single image captured by a confocal microscope. Middle column: A combination of an immunofluorescent detection of capillaries with the histochemical reaction for NADH-tetrazolium (TR) reductase. Very dark fibers are highly oxidative, and the pale fibers are non-oxidative. Right column: 3D rendering of capillaries and muscle fiber types: highly oxidative fibers (dark blue), fibers with an intermediate activity (light blue), and fibers with very low NADH activity (white). Top row: control EDL muscle. Middle row: denervated EDL muscle. Bottom row: reinnervated EDL muscle. Bar = 50 μm.

regard to fiber diameter ($p<0.013$, $p<0.006$, and $p<0.004$, respectively), perimeter ($p<0.005$, $p<0.007$, and $p<0.001$, respectively), and cross-sectional area ($p<0.016$, $p<0.018$, and $p<0.001$, respectively; Figure 3).

Lcap/Lfib was nearly equal for O and G fibers in all three groups.

Lcap/Sfib and Lcap/Vfib were significantly larger in O fibers than in G fibers in control, denervated, and

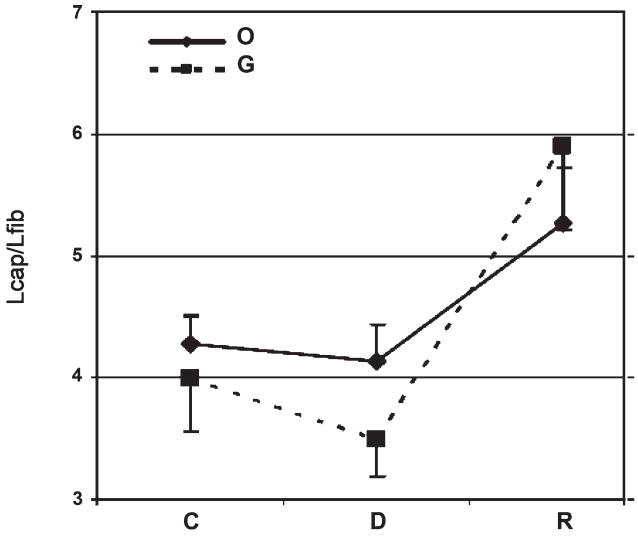

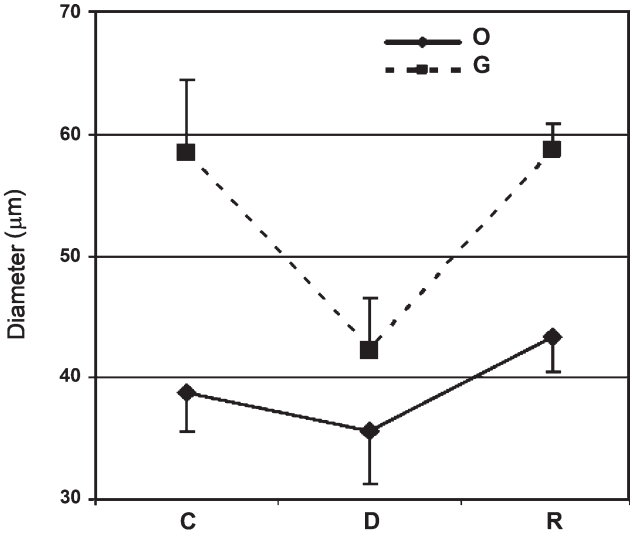

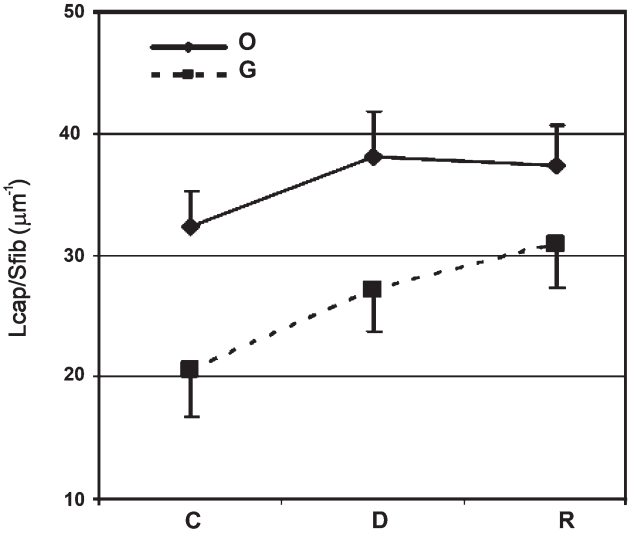

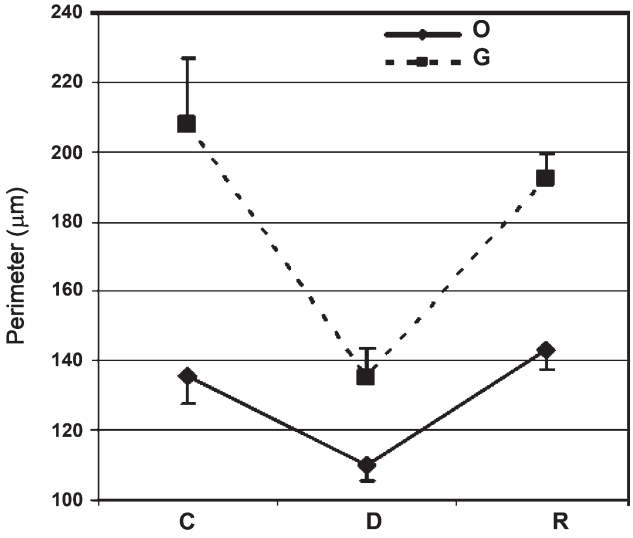

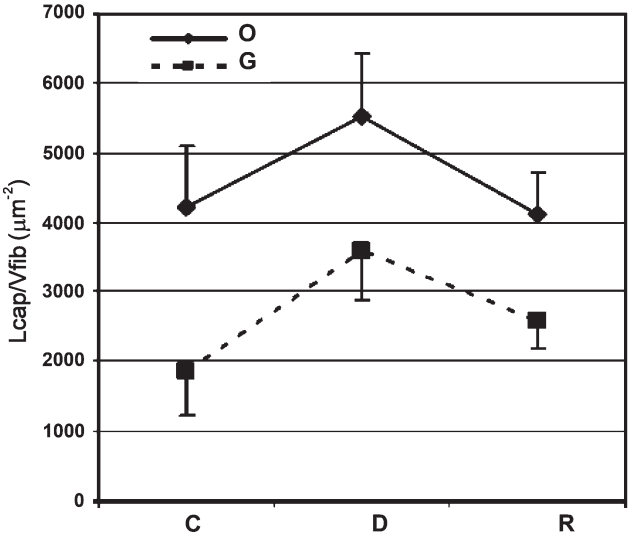

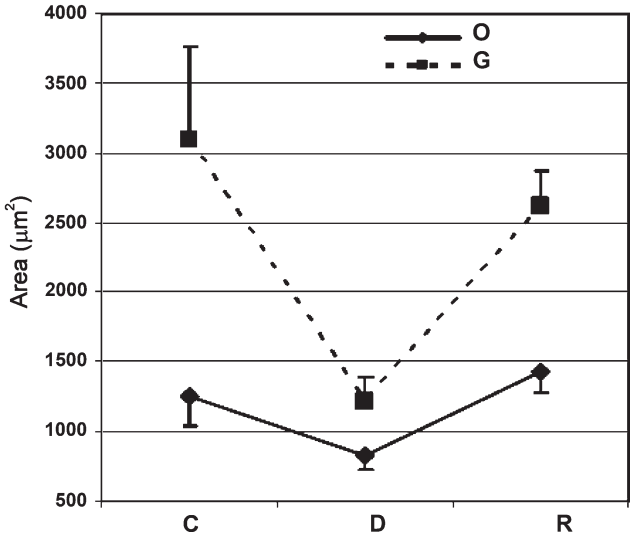

reinnervated EDL muscles ($p<0.001$, $p<0.005$, and $p<0.026$, respectively, for Lcap/Sfib; $p<0.001$, $p<0.001$, and $p<0.01$, respectively, for Lcap/Vfib).

Regression analysis confirmed that, in all animal groups, Lcap/Vfib decreased with increasing fiber cross-sectional area in both oxidative ($R^2 = 0.4345$, $p<0.0001$, $n=149$ in control, $R^2 = 0.307$, $p<0.0001$, $n=136$ in denervated, $R^2 = 0.5442$, $p<0.0001$, $n=107$ in reinnervated EDL) and non-oxidative fibers ($R^2 = 0.6064$, $p<0.0001$, $n=130$ in control, $R^2 = 0.4869$, $p<0.0001$, $n=127$ in denervated, $R^2 = 0.3069$, $p<0.0001$, $n=100$ in reinnervated EDL; Figure 4). The relation between the fiber perimeter and Lcap/Sfib in control, denervated, and reinnervated muscle was less consistent. Lcap/Sfib decreased with increasing fiber perimeter in both fiber types in control EDL muscles ($R^2 = 0.0634$, $p<0.002$, $n=149$ for oxidative fibers, $R^2 = 0.3634$, $p<0.0001$, $n=130$ for non-oxidative fibers). In denervated EDL muscle, a significant relation was found in non-oxidative fibers only ($R^2 = 0.2863$, $p<0.0001$, $n=127$) and in reinnervated EDL muscle in oxidative fibers only ($R^2 = 0.1684$, $p<0.0001$, $n=107$; Figure 4).

Discussion

This study presented a combined histochemical technique that enables measuring the length of capillaries adjacent to fibers with a defined oxidative potential within a stack of completely registered images, captured by a confocal microscope. By tracing of capillaries within the defined volume of muscle tissue, a 3D rendering of capillaries and muscle fiber types is achieved. The method was applied to rat EDL muscle that underwent acute denervation and early reinnervation.

Capillaries and muscle fiber types were shown with a combination of the triple immunofluorescent method developed for confocal microscopy (Čebašek et al. 2004) and the histochemical method for NADH-dehydrogenase that was introduced in transmission microscopy (Novikoff et al. 1961). The advantage of the applied histochemical and morphometric methods is that the researcher can follow each individual capillary on its whole course in 3D space adjacent to a histochemically defined fiber. Because the staining of capillaries is not always continuous, tracing in 3D space is easier and quicker than marking intersections with every capillary profile in every virtual section, which was required in our previous studies where the slicer method was applied (Kubínová et al. 2001; Čebašek et al. 2005–2007). Additionally, the tracer method provides 3D visualization and yields comparable results with the slicer (Janáček et al. 2007). When marking intersections with virtual test planes used in the slicer (Kubínová et al. 2001), checking the course of every capillary in 3D is quite time consuming.

We measured the length of capillaries within 20-μm-thick stacks of images, although the maximal penetration of antibodies was from 20 to 60 μm. A further possibility to increase the dimension of the stack in z-axis could be registration of thick sections (cf. Karen et al. 2003; Čapek et al. 2009).

To show oxidative potential of a fiber, an NADH reaction was applied in this study. We are well aware that NADH is not the best enzyme for the discrimination of oxidative and non-oxidative fibers; however, it was not possible to combine the fluorescent staining of capillaries with succinate dehydrogenase (SDH). If we incubated for SDH before the capillary staining, the SDH reaction product was rinsed out from the tissue section, whereas after capillary staining, SDH demonstration failed because of the inactivation of the enzyme during the incubation procedure for the immunofluorescent demonstration of capillaries.

Nevertheless, we believe that the error in misclassification of muscle fibers caused by NADH compared with SDH was not very large. In our previous study (Čebašek et al. 2007), we showed that, in the EDL muscle of control rats and in reinnervated EDL muscle, identical fibers were stained with SDH and NADH. In denervated EDL muscle, ~10% more fibers were positive with NADH than with SDH, presumably because of the staining of the sarcoplasmic reticulum. Thorough analysis has also shown that, in denervated EDL muscle, 2× fibers were positive with NADH and negative with SDH.

Based on the hypothesis that oxidative fibers are better supplied with capillaries than non-oxidative fibers (Romanul 1965; Plyley and Groom 1975; Ingjer 1979), we separately measured the capillary network adjacent to oxidative fibers and capillaries around non-oxidative, presumably glycolytic fibers. Fiber types were defined according to the activity of the NADH reaction into three categories: (a) fibers with very high activity—oxidative fibers or fibers with a high oxidative potential (O); (b) fibers with intermediate activity; and (c) fibers with very low or none activity—glycolytic fibers or fibers with a low oxidative potential (G). Only two fiber groups, i.e., fibers with very high NADH activity and fibers with very low NADH activity, were analyzed

Figure 3 Capillary supply estimated by the length of capillaries per fiber length (Lcap/Lfib), the length of capillaries per fiber surface area (Lcap/Sfib), the length of capillaries per fiber volume (Lcap/Vfib), and morphometric characteristics (diameter, perimeter, and cross-sectional area) of highly oxidative (O) and non-oxidative (G) fibers in control (C), denervated (D), and reinnervated (R) rat EDL muscle (mean ± SD).

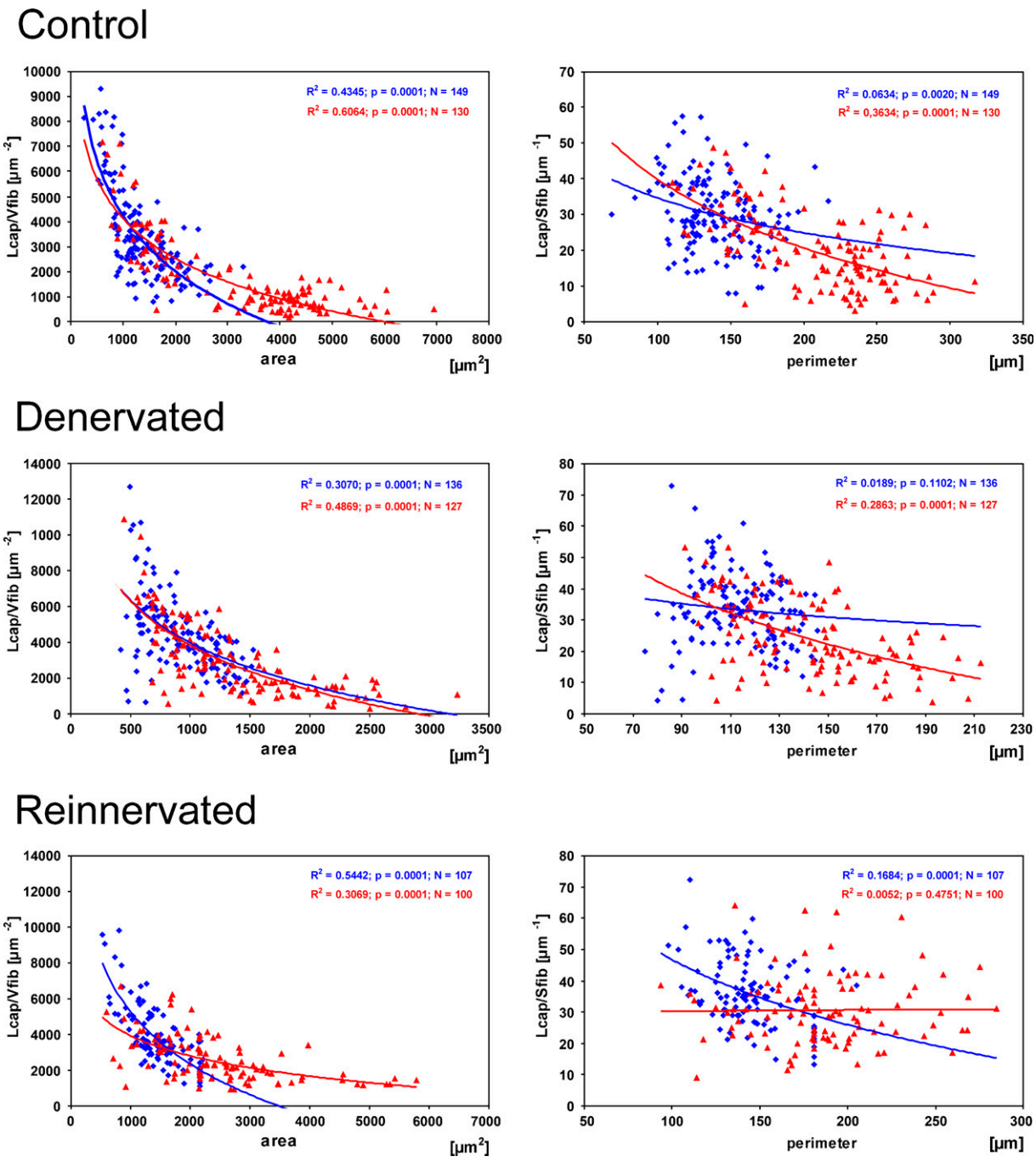

Figure 4 Correlation of the length of capillaries per fiber volume (Lcap/Vfib) with fiber cross-sectional area and the length of capillaries per fiber surface area (Lcap/Sfib) with fiber perimeter in highly oxidative (blue) and non-oxidative fibers (red) in control (top row), denervated (middle row), and reinnervated (bottom row) rat EDL muscle.

further. The NADH reaction could render a continuous spectrum of activities. Therefore, some fibers with intermediate activity could be assigned either to fibers with high activity or to fibers with very low activity. The extent of overlapping probably varied among animals and consequently increased the variability of the results.

Larger values of Lcap/Sfib and Lcap/Vfib that we obtained around O compared with G fibers in all experimental groups speak in favor of the hypothesis that, in a given muscle, oxidative fibers are anatomically better supplied with capillaries than non-oxidative fibers. Consistent with Egginton (1990) in rat EDL muscle, O

fibers were also smaller than G fibers (Figure 3). Despite the huge interindividual variability in fiber size, especially in the reinnervated muscle, a paired *t*-test proved that a significant difference in fiber size among the two fiber types persisted in all experimental groups. The difference in fiber girth between both fiber types was the smallest in the denervated group, presumably because of a more pronounced atrophy of IIX and IIB than type I and IIA fibers (Čebašek et al. 2007). The former two were also bigger in control muscles than the latter two. Furthermore, some fibers probably changed their histochemical profile from oxidative to non-oxidative. Whether the capillary network supplying these few fibers changed during the process of adapting the metabolic profile is difficult to judge. In our previous studies (Čebašek et al. 2006,2007), we reported that Lcap/Lfib of an average muscle fiber in the EDL muscle was maintained in the process of acute denervation and early reinnervation, although the variability between muscles in different experimental groups was quite high. Differences in Lcap/Sfib and Lcap/Vfib between experimental groups most probably originated from changes in muscle fiber girth.

In this study, capillary density estimated by Lcap/Lfib did not differ significantly between O and G fibers in any experimental group (Figure 3). This is in contrast with the early study of Romanul (1965), who reported that more capillary profiles exist around oxidative fibers than around non-oxidative fibers. Results provided by his methodological approach, i.e., counting capillary profiles around individual fibers (CAF) in single 2D images, are to some extent comparable to the 3D measurement of the length of capillaries surrounding a fiber per unit fiber length (Lcap/Lfib) applied in this study. In contrast to CAF, Lcap/Lfib did not show any significant difference between the two fiber types.

Assuming that the rate of oxygen diffusion through the capillary wall into individual muscle fibers depends only on the pressure gradient at an equal Lcap/Lfib, fibers with smaller girth are better oxygenated than fibers with larger girth, i.e., smaller fibers are anatomically better supplied with capillaries than larger fibers. Although Lcap/Sfib and Lcap/Vfib, which we measured, were larger in O fibers than in G fibers (Figure 3) in all experimental groups, this is not sufficient proof for the conclusion that all O fibers are supplied by a denser capillary network than G fibers. Degens et al. (2006) proved that capillary spacing is maintained during muscle growth to preserve the potential for adequate intramuscular oxygenation. In rat EDL muscle, the difference in size between both fiber types is preserved in all three groups, whereas Lcap/Lfib is not significantly different. Larger values of Lcap/Sfib and Lcap/Vfib show better capillary supply of oxidative fibers, thus reflecting changes in fiber size. The results of Egginton (2002) in the tibialis anterior muscle of normothermic and hypothermic rats and hamsters, as well as data from Panisello et al. (2008) obtained in tibialis anterior and diaphragm muscles in control rats and animals exposed to intermittent hypoxia, showed the same trend. Moreover, a general decrease in Lcap/Sfib and Lcap/Vfib with increasing fiber girth that concerns both O and G fibers in this study (Figure 4) and positive correlation of local capillary-to-fiber ratio (LCFR) with fiber area, which was independent of fiber type in human muscles (Ahmed et al. 1997), speak in favor of the hypothesis that capillary supply is primarily scaled to fiber size and is relatively independent of fiber type.

It is not clear whether remodeling equally affected the capillary network adjacent to all muscle fibers. However, if the capillary density was adjusted differently around different fiber types, this eventual differential remodeling was not extensive enough to contribute to statistically significant differences among fiber types. Nevertheless, it is not excluded that, in certain physiological or experimental conditions (Gute et al. 1994; Badr et al. 2003), remodeling of the capillary network attacks only capillaries that supply certain fibers or fiber types, although it is still not clear whether the main reason for angiogenesis is adaptation in fiber type or more probably changes in fiber size.

Egginton and Hudlicka (2000) have shown that, additional to the key role that capillaries play in oxygen transport, other factors such as waste removal may result in an increased capillary supply in the glycolytic regions of rat skeletal muscles that is not accompanied by changes in oxidative capacity. Badr et al. (2003) showed that, during angiogenesis induced by mechanical stimuli, capillary growth occurred specifically around fibers in glycolytic regions. The reason for this could be that glycolytic fibers, which have twice the girth of oxidative fibers in rat muscle and are usually supplied by fewer capillaries, may become relatively hypoxic following an increase in metabolic demand (Deveci et al. 2001).

Finally, differences in capillary density exist among different muscles, independent of the parameter of estimation that is applied (cf. Romanul 1965; Capo and Sillau 1983; Degens et al. 1992,2006; Stål et al. 1996; Čebašek et al. 2005,2006). Our previous results (Čebašek et al. 2005) showed an ~1.5-fold difference in Lcap/Lfib between rat soleus and EDL muscles. This result corresponds well with the data obtained in rabbit red and white muscle fibers (Gray and Renkin 1978). However, in control rat EDL muscle, there was no difference either between the smallest and largest fibers (Čebašek et al. 2005) or between highly oxidative and non-oxidative fibers (this study).

When capillary density was reported to differ among fiber types in a muscle, it was usually because of differences in fiber size. The existing difference in size could

be reduced or enlarged because of the selective atrophy or hypertrophy of particular fiber types provoked by different experimental and physiological conditions.

In conclusion, muscle capillary supply in the rat EDL muscle seems to be primarily scaled according to fiber size and is relatively independent of muscle fiber oxidative potential, which is similar to that suggested for human muscles (Ahmed et al. 1997). Therefore, in the EDL muscle, differences in capillarity among fiber types and better capillary supply of fibers with a very high oxidative potential compared with fibers with a very low oxidative potential are not reflected in Lcap/Lfib, are presumably not in the number of capillaries per fiber or in the number of capillaries around a fiber, but are much better described by Lcap/Sfib and Lcap/Vfib. However, this explanation holds true only for the rat EDL muscle. The capillary network of muscle fibers in other skeletal muscles may adapt differently to denervation and reinnervation.

Acknowledgments

This study was financially supported by the Slovenian Research Agency and the Ministry of Education, Youth and Sports of the Czech Republic (KONTAKT Grant MEB 090606 and Grant LC06063) and by the Grant Agency of Academy of Sciences of the Czech Republic (Grant A100110502).

We thank Prof. Marko Kreft for his help with the confocal microscope at the Institute for Pathophysiology in Ljubljana. Technical support from Majda Črnak Maasarani, Marko Slak, and Milan Števanec is greatly appreciated.

Literature Cited

Adolfson J, Ljungquist A, Tornling G, Unge G (1981) Capillary increase in the skeletal muscle of trained young and adult rats. J Physiol 310:529–532

Ahmed SK, Egginton S, Jakeman PM, Mannion AF, Ross HF (1997) Is human skeletal muscle capillary supply modelled according to fibre size or fibre type? Exp Physiol 82:231–234

Andersen P, Henricksson J (1977) Capillary supply of the quadriceps femoris muscle of man: adaptive response to exercise. J Physiol 270:677–690

Badr I, Brown MD, Egginton S, Hudlicka O, Milkiewicz M, Verhaeg J (2003) Differences in local environment determine the site of physiological angiogenesis in rat skeletal muscle. Exp Physiol 88:565–568

Brodal P, Ingjer F, Hermansen L (1977) Capillary supply of skeletal muscles fibers in untrained and endurance trained men. Am J Physiol 232:H7705–7712

Brown MD, Cotter MA, Hudlicka O, Vrbova G (1976) The effects of different patterns of muscle activity on capillary density, mechanical properties and structure of slow and fast rabbit muscles. Pflugers Arch 361:241–250

Čapek M, Brůža P, Janáček J, Karen P, Kubinová L, Vagnerová R (2009) Volume reconstruction of large tissue specimens from serial physical sections using confocal microscopy and correction of cutting deformations by elastic registration. Microsc Res Tech 72:110–119

Capo LA, Sillau AH (1983) The effect of hypothyroidism on capillarity and oxidative capacity in rat soleus and gastrocnemius muscles. J Physiol 342:1–14

Čebašek V, Kubínová L, Janáček J, Ribarič S, Eržen I (2007) Adaptation of muscle fiber types and capillary network to acute denervation and shortlasting reinnervation. Cell Tissue Res 330:279–289

Čebašek V, Kubínová L, Ribarič S, Eržen I (2004) A novel staining method for quantification and 3D visualisation of capillaries and muscle fibres. Eur J Histochem 48:151–158

Čebašek V, Kubínová L, Ribarič S, Eržen I (2005) Capillary network in slow and fast muscles and in oxidative and glycolytic muscle fibres. Image Anal Stereol 24:51–58

Čebašek V, Radochová B, Kubínová L, Ribarič S, Eržen I (2006) Nerve injury affects the capillary supply in rat slow and fast muscles differently. Cell Tissue Res 323:305–312

Charifi N, Kadi F, Feasson L, Costes F, Geyssant A, Denis C (2003) Enhancement of microvessel tortuosity in the vastus lateralis muscle of old men in response to endurance training. J Physiol 554:559–569

Cotter MA, Hudlicka O, Pette D, Staudte H, Vrbova H (1973) Changes of capillary density and enzyme pattern in fast rabbit muscles during long-term stimulation. J Physiol 230:34P–35P

Degens H, Deveci D, van Bemden AB, Hoofd LJC, Eginton S (2006) Maintenance of heterogeneity of capillary spacing is essential for adequate oxygenation in the soleus muscle of the growing rat. Microcirculation 13:467–476

Degens H, Turek Z, Hoofd LJC, van't Hof MA (1992) The relationship between capillarisation and fibre types during compensatory hypertrophy of the plantaris muscle in the rat. J Anat 180:455–463

Deveci D, Marshall JM, Egginton S (2001) Relationship between capillary angiogenesis, fibre type and fibre size in chronic systemic hypoxia. Am J Physiol Heart Circ Physiol 281:H241–255

Egginton S (1990) Numerical and areal density estimates of fibre type composition in a skeletal muscle (extensor digitorum longus). J Anat 168:73–80

Egginton S (2002) Temperature and angiogenesis. The possible role of mechanical factors in capillary growth. Comp Biochem Physiol A Mol Integr Physiol 132:773–787

Egginton S, Hudlicka O (2000) Selective long term electrical stimulation of fast glycolytic fibres increases capillary supply but oxidative enzyme activity in rat skeletal muscles. Exp Physiol 85:567–573

Gray SD, Renkin EM (1978) Microvascular supply in relation to fibre metabolic type in mixed skeletal muscles of rabbits. Microvasc Res 16:406–425

Gute D, Laughin MH, Amann JF (1994) Regional changes in capillary supply in skeletal muscle of interval-sprint and low-intensity, endurance-trained rats. Microcirculation 1:183–193

Hepple RT, Mathieu-Costello O (2001) Estimating the size of the capillary to fiber interface in skeletal muscle: a comparison of methods. J Appl Physiol 91:2150–2156

Hepple RT, Vogel JE (2004) Anatomic capillarization is maintained in relative excess of fiber oxidative capacity in some skeletal muscles of late middle-aged rats. J Appl Physiol 96:2257–2264

Ingjer F (1979) Effect of endurance training on muscle fibre ATPase activity, capillary supply and mitochondria content in man. J Physiol 294:419–432

Janáček J, Saxl I, Mao XW, Kubínová L (2007) Measurement of capillary length from 3D confocal images using image analysis and stereology. Focus on Microscopy, Valencia, Spain, April 10–13, Program and Abstract Book, p. 71

Karen P, Jirkovská M, Tomori Z, Demjénová E, Janáček J, Kubínová L (2003) Three-dimensional computer reconstruction of large tissue volumes based on composing series of high-resolution confocal images by GlueMRC and LinkMRC software. Microsc Res Tech 62:415–422

Kubínová L, Janáček J, Ribarič S, Čebašek V, Eržen I (2001) Three-dimensional study of the capillary supply of skeletal muscle fibres using confocal microscopy. J Muscle Res Cell Motil 22:217–227

Large J, Tyler KR (1985) Changes in capillary distribution in rat fast muscles following nerve crush and reinnervation. J Physiol 362: 13–21

Mai JV, Edgerton VR, Barnard RJ (1970) Capillarity of red, white and intermediate muscle fibers in trained and untrained guinea pigs. Experientia 26:1222–1223

Mathieu O, Cruz-Orive LM, Hoppeler H, Weibel ER (1983) Estimating length density and quantifying anisotropy in skeletal muscle capillaries. J Microsc 131:131–146

Maxwell LC, White TP, Faulkner JA (1980) Oxidative capacity, blood flow, and capillarity of skeletal muscles. J Appl Physiol 49:627–633
Novikoff AB, Shin WY, Drucker J (1961) Mitochondrial localization of oxidative enzymes: staining results with two tetrazolium salts. J Biophys Biochem Cytol 9:47–61
Panisello P, Torell JR, Esteva S, Pages T, Viscor G (2008) Capillary supply, fibre types and fibre morphometry in rat tibialis anterior and diaphragm muscle after intermittent exposure to hypobaric hypoxia. Eur J Appl Physiol 103:203–213
Plyley MJ, Groom AC (1975) Geometrical distribution of capillaries in mammalian striated muscle. Am J Physiol 228:1376–1383
Poole DC, Mathieu-Costello O, West JB (1989) Capillary tortuosity in rat soleus muscle is not affected by endurance training. Am J Physiol 256:H1110–1116
Ribarič S, Stefanovska A, Brzin M, Kogovšek M, Krošelj P (1991) Biochemical, morphological, and functional changes during peripheral nerve regeneration. Mol Chem Neuropathol 15:143–157
Romanul FCA (1965) Capillary supply and metabolism of muscle fibers. Arch Neurol 12:497–509
Romanul FCA, Pollock M (1969) The parallelism of changes in oxidative metabolism and capillary supply of skeletal muscle fibers. In Locke S, ed. Modern Neurology. Boston, Little Brown, 203–213
Sillau AH (1985) Capillarity, oxidative capacity and fibre composition of the soleus and gastrocnemius muscles of rats in hypothyroidism. J Physiol 361:281–295
Sillau AH, Aquin L, Lechner A, Bui MV, Banchero N (1980) Increased capillary supply in skeletal muscle of guinea pigs acclimated to cold. Respir Physiol 42:233–245
Škorjanc D, Jaschinsky F, Heine G, Pette D (1998) Sequential increases in capillarization and mitochondrial enzymes in low-frequency-stimulated rabbit muscle. Am J Physiol 274:C810–818
Stål P, Eriksson P-O, Thornell LE (1996) Differences in capillary supply between human oro-facial, masticatory and limb muscles. J Muscle Res Cell Motil 17:183–197
Sullivan SM, Pitman RN (1984) In vitro O_2 uptake and histochemical fiber type of resting hamster muscles. J Appl Physiol 57:246–253
Ziada AMA, Hudlicka O, Tyler KR, Wright AJA (1984) The effect of long-term vasodilatation on capillary growth and performance in rabbit heart and skeletal muscle. Cardiovasc Res 18: 724–732

The Journal of Histochemistry & Cytochemistry